IEEE Access
Multidisciplinary : Rapid Review : Open Access Journal

Received June 18, 2019, accepted August 5, 2019, date of publication August 9, 2019, date of current version August 26, 2019.

Digital Object Identifier 10.1109/ACCESS.2019.2934156

Isolation Enhancement for Wideband, Circularly/Dual-Polarized, High-Density Patch Arrays Using Planar Parasitic Resonators

ZHIYUAN CHEN[1], (Student Member, IEEE), MEI LI[1], (Member, IEEE), GUO LIU[2], ZHENTIAN WU[1], AND MING-CHUN TANG[1], (Senior Member, IEEE)

[1]Key Laboratory of Dependable Service Computing in Cyber Physical Society Ministry of Education, School of Microelectronics and Communication Engineering, Chongqing University, Chongqing 400044, China

[2]Science and Technology on Electronic Information Control Laboratory, Chengdu 610036, China

Corresponding author: Mei Li (li.mei@cqu.edu.cn)

This work was supported in part by the National Natural Science Foundation of China under Contract 61701052, in part by the Graduate Scientific Research and Innovation Foundation of Chongqing, China, under Contract CYB18069, in part by the Funding of the Science and Technology on Electronic Information Control Laboratory under Contract JS20190500058, in part by the Funding of the Innovative Leading Talents in Science and Technology of Chongqing under Contract CSTCCXLJRC201705, in part by the Funding of the Leading Research Talent Cultivation Plan of Chongqing University under Contract cqu2017hbrc1A08, in part by the Funding of the Young Backbone Teachers in Colleges and Universities of Chongqing under Contract 0307001104102, and in part by the Fundamental Research Funds for the Central Universities under Contract 2018CDQYTX0025.

ABSTRACT A planar double-layer hybrid decoupling structure with the polarization-insensitive characteristics is proposed as an effective isolator for wideband, circularly/dual-polarized, high-density patch arrays. The hybrid decoupling structure is composed of two types of resonators, i.e., an H-shaped structure on the lower layer and a couple of meander lines on the upper layer. By integrating the decoupling structure into the dual-polarized array and circularly polarized array, respectively, the mutual coupling between the antenna elements is significantly reduced. In detail, the isolation levels between the co-polarization (co-pol) ports in dual-polarized array are improved by ~ 9.40 dB and the port isolation level in circularly polarized (CP) array is improved by ~ 12.7 dB, while the inter-element center-to-center distances are as low as 0.5 λ_0. Good agreement between the simulated results and the measured results is obtained.

INDEX TERMS Dual-polarized array, circularly polarized array, high-density array, mutual coupling reduction.

I. INTRODUCTION

With the advancements in communication technology, the demand for high data rate and large-channel capacity has increased significantly for the applications of various mobile wireless communication devices. It requires allocating as many radiators as possible to meet the communication demands in a quite limited space. As an effective solution, dual-polarized antennas contain two ports which demonstrate the polarizations orthogonal to each other, thus making them operate independently without affecting each other's performance. This dual-polarization operation mechanism empowers one radiator to hold two radiators' functions, thus to save much space [1], [2]. Furtherly, in order to save more space, one can place the dual-polarized antennas very close to construct the high-density array. However, the small spacing between adjacent elements would inevitably result in very strong inter-element mutual coupling, which would seriously deteriorate the radiation pattern, radiation efficiency, impedance matching, etc [3]. Therefore, it is important to reduce the mutual coupling in high-density dual-polarized arrays.

Compared with the single-polarized antenna arrays, the coupling mechanism of the dual-polarized arrays is much more complicated, because there exists both the electrical coupling and magnetic coupling between elements. Recently, few works about reducing the mutual coupling between dual-polarized array elements were reported. For example,

The associate editor coordinating the review of this article and approving it for publication was Derek Abbott.

a dual-polarized magnetically coupled patch antenna array with high port isolation was presented in [4]. In the design, a pair of metal cavities and an artificial periodic structure (APS) composed of metal strips etched vertically on the ground plane were used to improve the port isolations between array elements. In [5], an array-antenna decoupling surface (ADS) was proposed for the compact dual-polarized array decoupling. The ADS is composed of a plurality of electrically small metal patches and is placed above the array antenna to create partial reflective electromagnetic (EM) waves to cancel the coupled waves from the adjacent antenna elements to improve the isolation. In [6], a 3-dimensional (3-D) meta-structure was integrated into a high-density dual-polarized array for mutual coupling reduction. By incorporating the meta-structure into the dual polarized array, the isolation levels between adjacent radiating elements in both the E- and H- plane orientations could be improved significantly. However, the inherent drawbacks associated with above techniques may occur to hinder their widespread applications, e. g., the employment of APS cannot reduce the inter-element spacing ($\sim 1.3\lambda_0$) [4], the usage of the ADS requires relatively high profile (around one-quarter wavelength) and is not suitable for decoupling of circularly polarized (CP) arrays [5], and 3-D meta-structure was difficult to integrated into the antenna system [6], respectively.

In this study, a compact, wideband, planar, polarization insensitive, hybrid decoupling structure is presented. By integrating the planar structure into the high-density array, the mutual coupling between elements is significantly reduced.

II. EMPLOYMENT OF THE HYBRID STRUCTURE IN DUAL-POLARIZED ARRAY

As depicted in Fig. 1, one hybrid decoupling structure is integrated into a two-element dual-polarized antenna array. The center-to-center distance between the two elements (No. 1 and No. 2) is 0.5 λ_0, where λ_0 indicates the operational wavelength in the free space corresponding to the low frequency f_0. The hybrid decoupling structure has the advantages of planar configuration and easy of fabrication.

As is shown in Fig. 1(a), the hybrid decoupling structure comprises one H-shaped structure and a couple of meander lines, which are loaded halfway between the two antenna elements and placed above the array. Two layers of Taconic CER-10 dielectric substrates with the thickness of 1 mm, relative permittivity: $\varepsilon_r = 10$, and loss tangent: $\tan\delta = 0.0035$, are placed above the antenna array, namely Layer_1 and Layer_2. The meander lines are etched on the upper surface of the Layer_1, and the H-shaped structure is printed on the upper surface of the Layer_2. There are air-gaps between Layer_1 and Layer_2, between Layer_2 and Layer_3, and between Layer_3 and Layer_4 with the heights of $h_1 = 5.5$ mm, $h_2 = 9$ mm, and $h_3 = 7$ mm, respectively. On the Layer_3, a square radiating patch is printed on the top side of a Taconic CER-10 substrate with the thickness of 1 mm. The parasitic ground, which is etched with a pair of coupled slots, is printed on the upper surface of Layer_4. A pair of feeding strips and the metallic ground are printed on the top and bottom sides of Layer_5, respectively. Layer_4 and Layer_5, which are, respectively, with the thickness of 0.64 mm and 3.18mm, are constructed by Taconic RF-60 substrates that have the characteristics of $\varepsilon_r = 6.15$, $\tan\delta = 0.0028$. Additionally, a number of metallic vias with radius of 0.5 mm connect the parasitic ground and the bottom metallic ground. Finally, the 50 Ω Sub-Miniature-A (SMA) connectors are used to facilitate the connection between the feeding strips and sources. The parameter values of the optimized decoupling array are listed in Table 1.

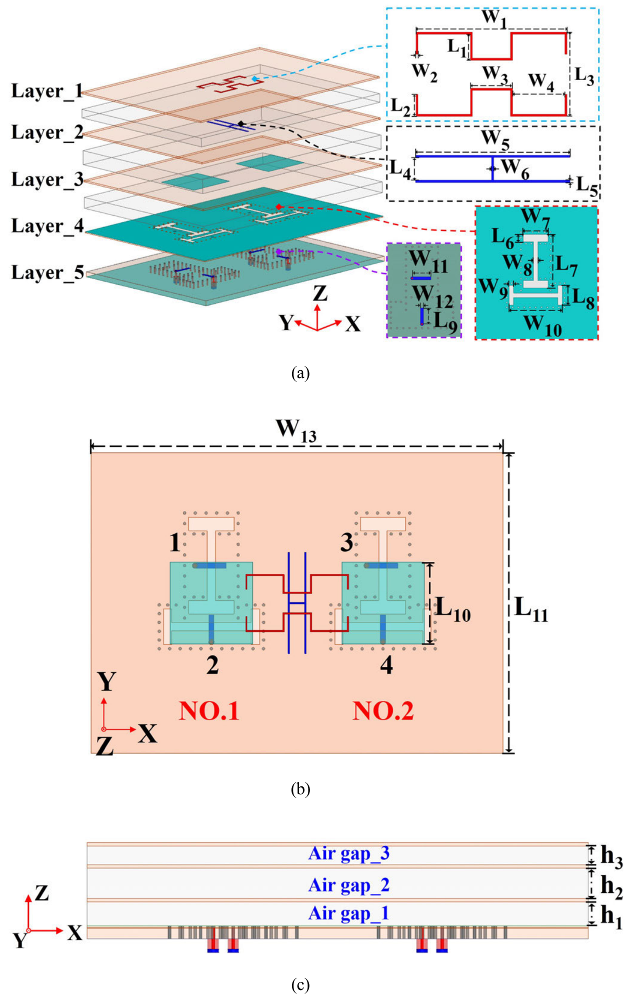

FIGURE 1. Two-element dual-polarized array loaded with the hybrid decoupling structure. (a) 3-D view of the array with its layers detached; (b) top view; (c) side view.

TABLE 1. Design parameters of the decoupling array (Unit: mm).

Parameter	L_1	L_2	L_3	L_4	L_5	L_6	L_7	L_8
Value	6.5	5.5	21	5.5	0.5	5	35.5	13
Parameter	L_9	L_{10}	L_{11}	W_1	W_2	W_3	W_4	W_5
Value	9.37	30	110	37.5	0.5	10.5	13	37.5
Parameter	W_6	W_7	W_8	W_9	W_{10}	W_{11}	W_{12}	W_{13}
Value	0.5	16.5	3	3	35	11	1.75	150

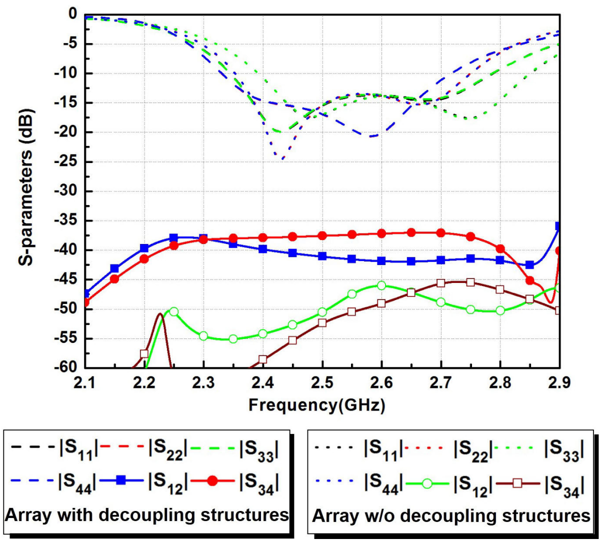

(a)

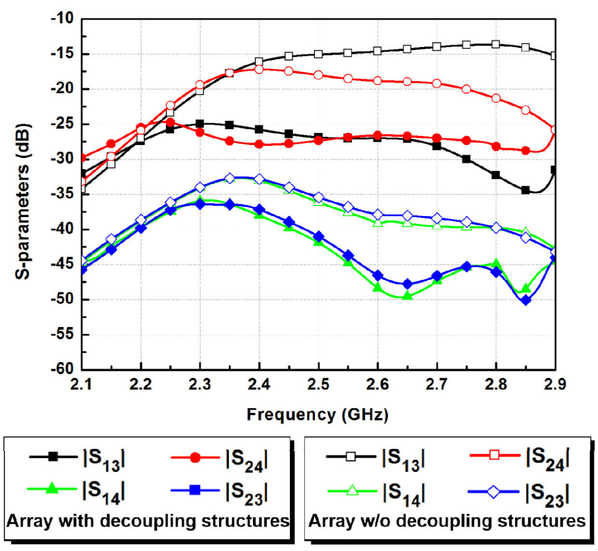

(b)

FIGURE 2. **Simulated reflection coefficients and port isolation levels for the array with and without the planar hybrid decoupling structure. (a) $|S_{12}|$, $|S_{34}|$ and reflection coefficients; (b) $|S_{13}|$, $|S_{14}|$, $|S_{23}|$ and $|S_{24}|$.**

A. MUTUAL COUPLING REDUCTION EVALUATIONS

The corresponding simulated reflection coefficients and port isolation levels for the two-element array with and without the planar hybrid decoupling structure are given in Fig2. As shown in Fig. 2(a), the working band (reflection coefficients < -10 dB) of the array in both cases covers the range of 2.4-2.7 GHz. Moreover, the mutual couplings between cross-polarization (cross-pol) ports for antenna elements NO.1 ($|S_{12}|$) and NO.2 ($|S_{34}|$) are kept at very low levels and all below -35 dB, which demonstrates that the planar hybrid decoupling structure has little effect on the S-parameters of each antenna elements.

The simulated isolations levels for both the co-polarization (co-pol) ports ($|S_{13}|$ and $|S_{24}|$) and the cross-pol ports in the cases of the two-element array with and without the planar hybrid decoupling structure are given in Fig. 2(b). By comparing the results in the two cases, it is apparent that the isolation levels between the co-pol ports of the two-element array could be improved significantly by loading with the planar hybrid decoupling structure. In particular, the maximum value of $|S_{13}|$ ($|S_{24}|$) over the entire operational band is decreased from -14.02 dB (-17.20 dB) to -25.79 dB (-26.44 dB), exhibiting $\sim$11.77 dB ($\sim$9.24 dB) improvement. Moreover, the isolations between the cross-pol ports ($|S_{23}|$ and $|S_{14}|$) are kept at very low levels in both cases when loaded with the planar hybrid decoupling structure. The results show that the proposed planar hybrid structure has an excellent decoupling effect on the compact dual-polarized array.

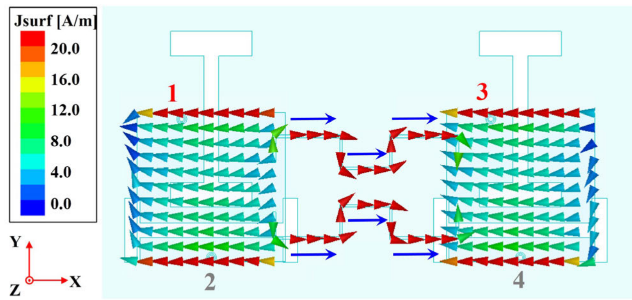

(a)

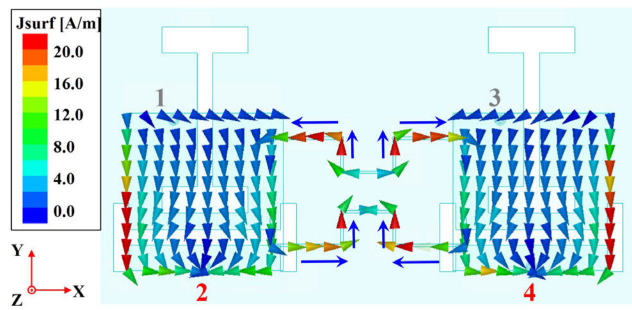

(b)

FIGURE 3. **Surface current distributions of the two-element array loaded only with a couple of meander lines. (a) Only ports 1 and 3 are excited; (b) Only ports 2 and 4 are excited. (The current polarizations on the meander lines are highlighted by the blue arrows).**

B. MUTUAL COUPLING REDUCTION MECHANISMS

As two types of the decoupling structures have quite different decoupling mechanisms, the following two cases when the array is with only one type of decoupling structure will be analyzed in a comprehensive manner. The surface current distributions on the traces of the two-element array loaded with only a couple of meander lines are shown in Fig. 3. When ports 1 and 3 are excited with the same amplitude and phase, the two antenna elements of the array are equivalent to be oriented along the E-plane. In this case, it is dominated by electrical coupling between ports 1 and 3. Obviously, very strong out-of-phase current is induced on the surface of the

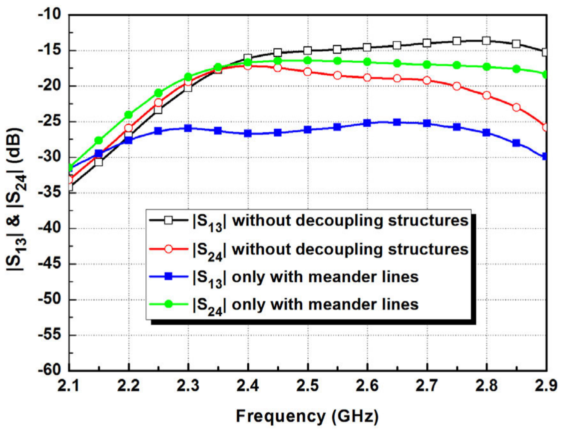

FIGURE 4. Simulated port isolations between the co-pol ports for the two-element array with only meander lines and the two-element array without decoupling structures.

meander lines. Since the coupling currents are offset to a great extent, the isolation level between the two ports was improved significantly. As shown in Fig. 4, the mutual coupling level between ports 1 and 3 is reduced from −14.02 dB to −25.06 dB, exhibiting 11.04 dB reduction. It should be noted that the meander lines can effectively increase the electrical length of the structure to ensure its physical size more compact for its application in high-density arrays. In contrast, when ports 2 and 4 are excited with the same amplitude and phase, the two antenna elements are equivalent to placing along the H-plane. Strong surface current on the meander lines also could be excited. However, the surface current on the meander lines is centrally symmetrical and out-of-phase with the almost equal amplitude. This current behavior resulted in a cancellation of their effects on the array, making the meander lines with the advantage of having a weak effect on the coupling between ports 2 and 4. As shown in Fig. 4, the simulated $|S_{24}|$ value demonstrates little fluctuation compared to the array without decoupling structure.

Similarly, Fig. 5 gives the current distributions when the two-element array loaded with only H-shaped decoupling structure. As illustrated in Fig. 5(a), when ports 1 and 3 are excited with the same amplitude and phase, which is equivalent to two E-plane-coupled antenna elements, strong surface current on the H-shaped strip could be excited. However, the surface current on the H-shaped strip is centrally symmetrical and out-of-phase with the almost equal amplitude. As a result, the coupling currents are canceled out to a great extent that makes the H-shaped structure have negligible influence on the mutual coupling level between ports 1 and 3. As shown in Fig. 6, the simulated $|S_{13}|$ value remains almost the same compared to that of the array without decoupling structures. In contrast, when ports 2 and 4 are excited with the same amplitude and phase, which is equivalent to the two H-plane-coupled antenna elements, strong out-of-phase current on the H-shaped strip could be induced, exhibiting a dipole resonance. Thus, the cancellation of coupling currents leads to a significant enhancement of the isolation level

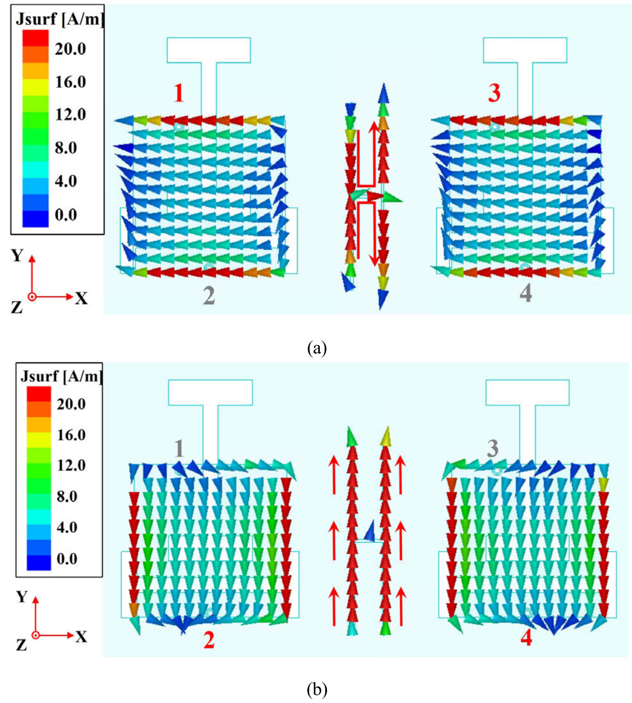

FIGURE 5. Surface current distributions of the two-element array loaded only with H-shaped structure. (a) Only ports 1 and 3 are excited; (b) Only ports 2 and 4 are excited. (The current polarizations on the H-shaped structure are highlighted by the red arrows).

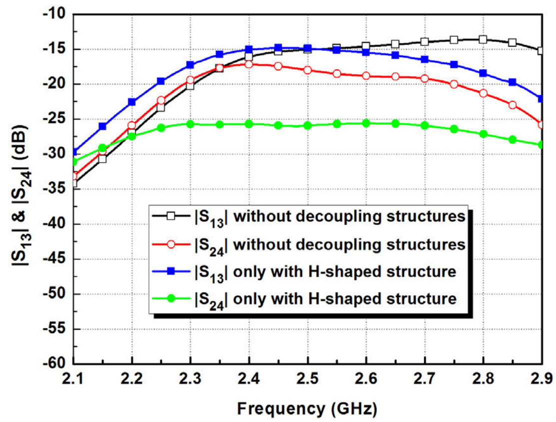

FIGURE 6. Simulated port isolations between the co-pol ports for the two-element array with only H-shaped structure and the two-element array without decoupling structures.

between ports 2 and 4. In detail, the $|S_{24}|$ value is reduced from the maximum −17.20 dB to −25.61 dB across the entire working band. This result fully manifests the effectiveness of the H-shaped structure for the decoupling of high-density arrays.

Since the proposed method could reduce the co-pol couplings between two radiators and in the same time maintain the low cross-pol coupling levels, it is quite different from the reported single-polarization decoupling methods, which include the use of parasitic elements [7]–[14], electromagnetic bandgap (EBG) structures [15]–[20], defected ground structures (DGSs) [21]–[26], metamaterial structures [27]–[30], neutralization lines [8], [31], [32], polarization-rotator [33], decoupling networks [34], [35], etc.

III. EMPLOYMENT OF THE HYBRID STRUCTURE IN CP ARRAY

As CP antennas have superior characteristics on signal propagation than linearly polarized counterparts [36], the usage of CP antenna arrays becomes popular in many applications. However, in CP arrays, strong mutual coupling not only deteriorates impedance matching, but also the polarization purity in terms of axial ratio (AR). Here, in order to further explore its wide application range, the proposed hybrid decoupling structure is applied into a high-density CP array to validate the polarization-insensitive characteristics.

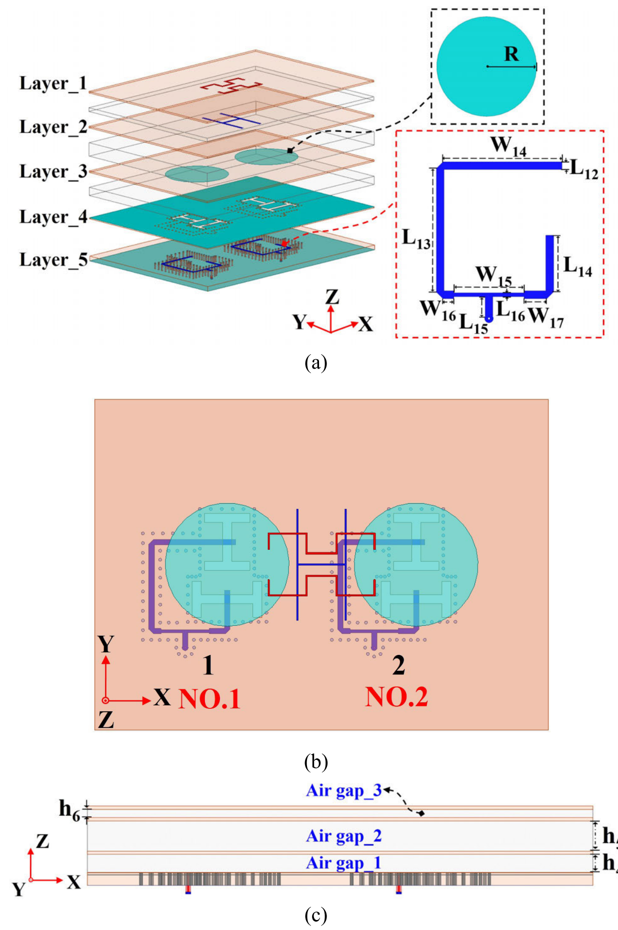

FIGURE 7. Two-element CP array loaded with the planar hybrid decoupling structure. (a) 3-D view of the array with its layers detached; (b) top view; (c) side view.

Fig. 7 depicts a two-element array, which consists of two CP elements, NO. 1 and NO. 2, with the center-to-center spacing 0.5 λ_0. The proposed decoupling structure is halfway placed between the two CP elements, similar to the dual-polarized array in Fig. 1. The material and thickness of the substrates in each layer are the same as those of the corresponding dual-polarized element. Note that, the radiator on the Layer_3 is selected to be circular patch according to the polarization characteristic of the CP antenna element. On the Layer_4, the geometrical parameter values of the pair of coupled slots are also fine-tuned. On the Layer_5, the feeding strip can form a 90° phase difference to generate CP wave. The 50 Ω SMA connectors are vertically connected to the feeding strip from the sources. The optimized geometrical parameter values of the array are listed in Table 2.

TABLE 2. Design parameters of the decoupling CP array (Unit: mm).

Parameter	R	L_1	L_2	L_3	L_4	L_5	L_6	L_7
Value	20	6.5	5.5	21	15.5	0.5	3	19
Parameter	L_8	L_{11}	L_{12}	L_{13}	L_{14}	L_{15}	L_{16}	W_1
Value	12	110	1.75	28.4	13	4.57	0.9	35.5
Parameter	W_2	W_3	W_4	W_5	W_6	W_7	W_8	W_9
Value	0.5	10.5	12	37	0.5	15	3	3
Parameter	W_{10}	W_{13}	W_{14}	W_{15}	W_{16}	W_{17}	h_4	h_5
Value	23	150	27.2	16	2.5	5.25	5.5	9
Parameter	h_6							
Value	2.5							

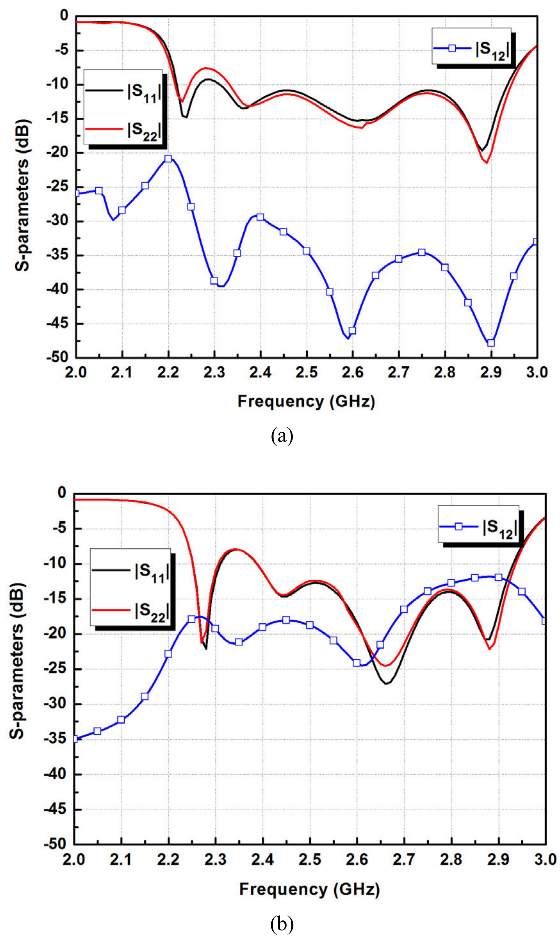

FIGURE 8. Simulated reflection coefficients and port isolation levels of the CP array. (a) With the planar hybrid decoupling structure; (b) without the planar hybrid decoupling structure.

The simulated S-parameter results of the optimized CP array with and without the planar hybrid structure are presented in Fig. 8. It is obvious that both the two elements

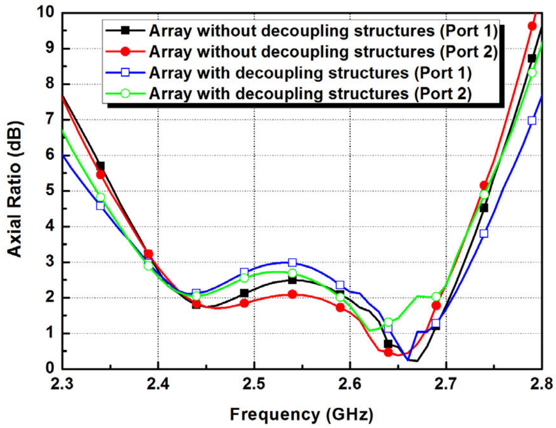

FIGURE 9. Simulated AR results for the two-element CP array with and without decoupling structures.

exhibit good impedance matching for the arrays with and without the decoupling structure. The operation band where the reflection coefficients < −10 dB covers the range of 2.4-2.7 GHz of our interest. Moreover, significant enhancement of the isolation level between the two CP elements could be achieved by loading with the planar hybrid decoupling structure. In detail, $|S_{12}|$ is decreased from −16.5 dB to −29.2 dB, witnessing ∼12.7 dB reduction. The simulated ARs for the arrays with and without the planar hybrid decoupling structure are given in Fig. 9. Apparently, the array maintains excellent CP characteristic (AR < 3 dB) in the entire operation frequency band.

The surface current distributions of the two-element CP array loaded with planar hybrid structure are shown in Fig. 10. When ports 1 and 2 are excited with the same amplitude and phase, it is clear that strong currents are also induced on the surface of the planar hybrid decoupling structure. By checking the current polarization over the entire period, it can be easily seen that, both the H-shaped strip and the meander lines are well induced. It should be mentioned that, at the fixed phase $\pi/4$, only the meander lines contribute the mutual coupling reduction, as is illustrated in Fig. 3. At the fixed phase $\pi/2$, only the H-shaped strip contributes the mutual reduction, as is illustrated in Fig. 5. At the rest phases, both the H-shaped strip and the meander lines collaborate to reduce the mutual coupling. This phenomenon indicates that the decoupling of the CP array is in fact the consequence of the collaboration of the two types of decoupling structures, which empowered the resulting hybrid decoupling structure to possess the unique advantage of polarization insensitivity.

IV. MEASUREMENT AND DISCUSSION

To further verify the effectiveness of the proposed planar hybrid decoupling structure, a two-element dual-polarized array loaded with both the H-shaped structure and a couple of meander lines was fabricated and measured. The antenna was fabricated using the low-cost multi-layer PCB processing technology. The photograph of the fabricated prototype is shown in Fig. 11. The corresponding S-parameters were

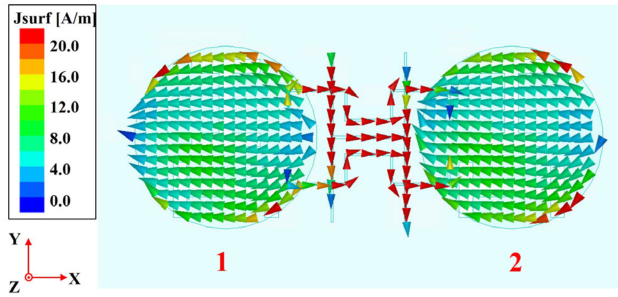

(a)

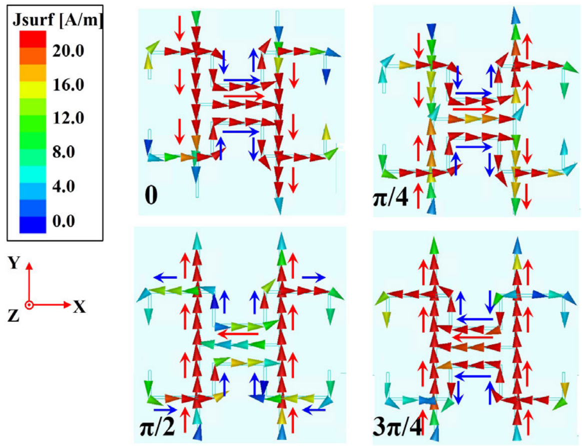

(b)

FIGURE 10. Surface current distributions. (a) Two-element CP array loaded with the planar hybrid decoupling structure; (b) only the planar hybrid decoupling structure under different excitation phases. (The current polarizations on the meander lines and the H-shaped structure are highlighted by the blue and red arrows, respectively).

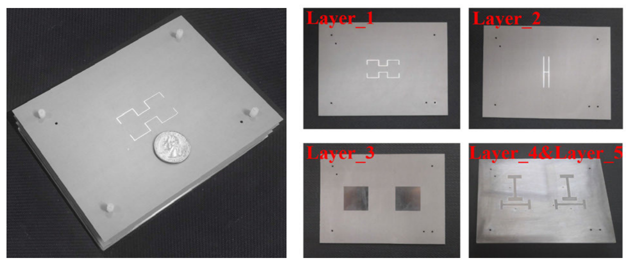

(a) (b)

FIGURE 11. The fabricated prototype of the two-element dual-polarized decoupling array. (a) 3-D view; (b) array before installation.

measured with an Agilent E8361A PNA vector network analyzer (VNA), and the far-field radiation performance characteristics were measured with a SATIMO passive measurement system at the Chongqing Academy of Information and Communications Technology (CAICT). The corresponding results are presented in Figs. 12 and 13.

As shown in Fig. 12(a), good impedance matching for all ports and high isolation levels between the cross-pol ports for each element are observed in the frequency band 2.4-2.7 GHz, where the reflection coefficients are less

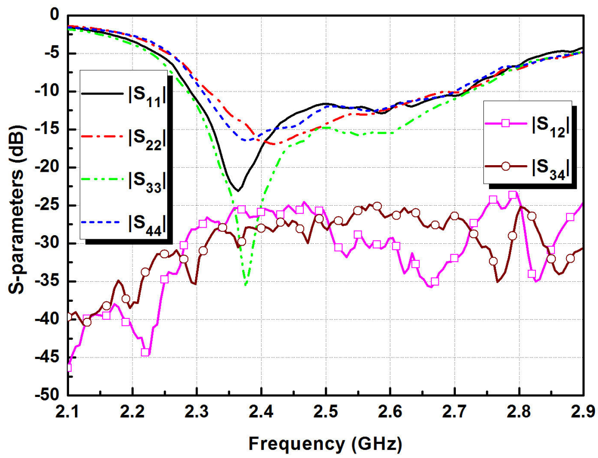

(a)

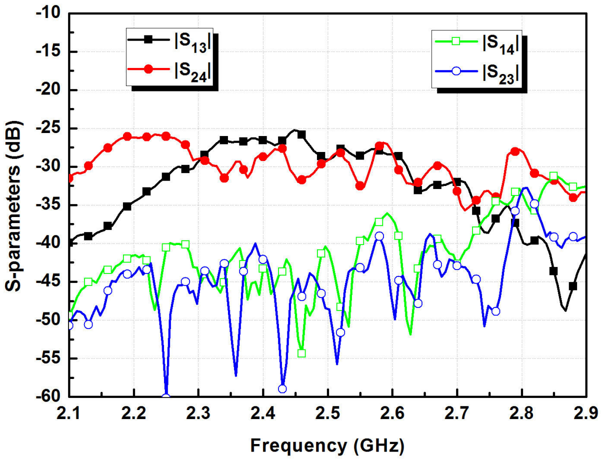

(b)

FIGURE 12. Measured reflection coefficients and port isolation levels for the decoupling array. (a) $|S_{12}|$, $|S_{34}|$ and reflection coefficients; (b) $|S_{13}|$, $|S_{14}|$, $|S_{23}|$ and $|S_{24}|$.

than −10 dB and $|S_{12}|$ and $|S_{34}|$ are lower than −35 dB. Next, Fig. 12(b) gives the mutual coupling levels for the co-pol ports ($|S_{13}|$ and $|S_{24}|$) between the two antenna elements as well as the cross-pol ports ($|S_{14}|$ and $|S_{23}|$). The mutual coupling levels for the co-pol ports remain below −25 dB, while the mutual coupling levels between the cross-pol ports maintain less than −35 dB.

The simulated and measured radiation patterns of the two-element array at 2.55 GHz, when only port 3 or port 4 is excited, are presented in Fig. 13. The measured (simulated) peak realized gains at the resonance frequency of 2.55 GHz are 7.4 dBi (7.22 dBi) and 8.75 dBi (9.15 dBi), respectively. Moreover, the measured (simulated) overall radiation efficiencies were as high as 84.1 % (97.7 %).

Overall, the measured results of the decoupling array are generally in good agreement with the simulated ones. Although there exists an acceptable difference, it could be attributed to inevitable processing tolerances and measurement errors.

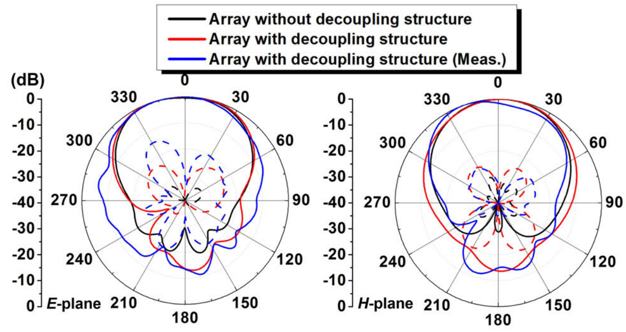

(a)

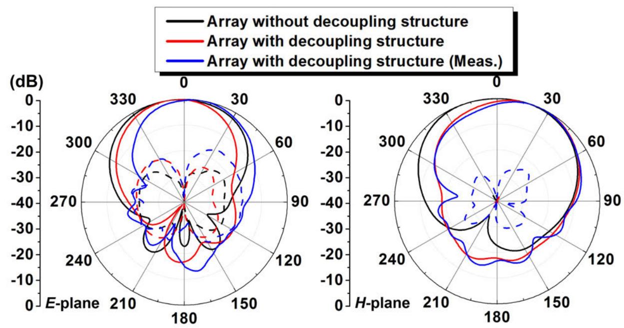

(b)

FIGURE 13. Simulated and measured radiation patterns of the two-element CP array at 2.55 GHz. (a) Only port 3 is excited; (b) only port 4 is excited.

TABLE 3. Performance comparison with some previous works.

Ref.	Configuration of Decoupling Structures	Element Separation (λ_0)	Operational Bandwidth (%)	Height (λ_0)	Array Type
[3]	2-D	0.28	1.0	0.025	S-L*
[4]	3-D	1.3	15.4	0.18	D-L*
[5]	2-D	0.5	14.1	0.275	D-L
[6]	3-D	0.6	8.7	0.213	D-L
[10]	2-D	0.83	~3.0	0.019	S-L
[19]	2-D	0.51	2.5	0.017	S-L
[30]	2-D	1.89	16.9	0.047	S-L
[33]	3-D	0.5	11.8	0.38	S-L
Proposed work	2-D	0.5	11.8	0.227	D-L/ C-P*

*S-L is the abbreviation of single-linear polarization, D-L of dual-linear polarization, and C-P of circular polarization

Table 3 provides the comparison between recent related methods in mutual coupling suppression and the proposed decoupling strategy in a comprehensive manner. For fair comparison, it includes the decoupling structure configurations, element separations, operational bandwidths, heights, and array types. Compared with the recent reported methods, the proposed hybrid structure not only exhibits wideband and polarization-insensitive (both dual-LP and CP) performance characteristics [3], [10], [19], [30], [33], but also demonstrates its simple, compact, low-profile, and easy-to-integrate configurations [4]–[6], which enables its widespread applications into the future various high-density arrays. In addition, we have verified that the proposed decoupling structure is applicable to patch arrays, which further demonstrates its widespread applicable characteristic.

V. CONCLUSION

The proposed hybrid decoupling structure, which consists of two planar decoupling structures, i.e., the H-shaped strip and a couple of meander lines, has been demonstrated as a tenable polarization-insensitive tool to reduce the mutual coupling in high-density patch antenna arrays. The decoupling mechanism of each planar structure was elaborated by investigating the surface current distributions. A principle prototype was fabricated and measured. The measured results were in good agreement with the simulated ones, validating the effectiveness of the proposed decoupling structure.

REFERENCES

[1] D. M. Pozar and S. D. Targonski, "A shared-aperture dual-band dual-polarized microstrip array," *IEEE Trans. Antennas Propag.*, vol. 49, no. 2, pp. 150–157, Feb. 2001.

[2] S.-G. Zhou, G.-L. Huang, T.-H. Chio, J.-J. Yang, and G. Wei, "Design of a wideband dual-polarization full-corporate waveguide feed antenna array," *IEEE Trans. Antennas Propag.*, vol. 63, no. 11, pp. 4775–4782, Nov. 2015.

[3] S. Hwangbo, H. Y. Yang, and Y.-K. Yoon, "Mutual coupling reduction using micromachined complementary meander-line slots for a patch array antenna," *IEEE Antennas Wireless Propag. Lett.*, vol. 16, pp. 1667–1670, 2017.

[4] J. Li, S. Yang, Y. Gou, J. Hu, and Z. Nie, "Wideband dual-polarized magnetically coupled patch antenna array with high port isolation," *IEEE Trans. Antennas Propag.*, vol. 64, no. 1, pp. 3872–3875, Jan. 2016.

[5] K.-L. Wu, C. Wei, X. Mei, and Z.-Y. Zhang, "Array-antenna decoupling surface," *IEEE Trans. Antennas Propag.*, vol. 65, no. 12, pp. 6728–6738, Dec. 2017.

[6] M.-C. Tang, Z. Chen, H. Wang, M. Li, B. Luo, J. Wang, Z. Shi, and R. W. Ziolkowski, "Mutual coupling reduction using meta-structures for wideband, dual-polarized, and high-density patch arrays," *IEEE Trans. Antennas Propag.*, vol. 65, no. 8, pp. 3986–3998, Aug. 2017.

[7] Z. Li, Z. Du, M. Takahashi, K. Saito, and K. Ito, "Reducing mutual coupling of MIMO antennas with parasitic elements for mobile terminals," *IEEE Trans. Antennas Propag.*, vol. 60, no. 2, pp. 473–481, Feb. 2012.

[8] X. Ling and R. Li, "A novel dual-band MIMO antenna array with low mutual coupling for portable wireless devices," *IEEE Antennas Wireless Propag. Lett.*, vol. 10, pp. 1039–1042, 2011.

[9] B. K. Lau and J. B. Andersen, "Simple and efficient decoupling of compact arrays with parasitic scatterers," *IEEE Trans. Antennas Propag.*, vol. 60, no. 2, pp. 464–472, Feb. 2012.

[10] K. S. Vishvaksenan, K. Mithra, R. Kalaiarasan, and K. S. Raj, "Mutual coupling reduction in microstrip patch antenna arrays using parallel coupled-line resonators," *IEEE Antennas Wireless Propag. Lett.*, vol. 16, pp. 2146–2149, 2017.

[11] A. C. K. Mak, C. R. Rowell, and R. D. Murch, "Isolation enhancement between two closely packed antennas," *IEEE Trans. Antennas Propag.*, vol. 56, no. 11, pp. 3411–3419, Nov. 2008.

[12] J.-H. Xun, L.-F. Shi, W.-R. Liu, G.-X. Liu, and S. Chen, "Compact dual-band decoupling structure for improving mutual coupling of closely placed PIFAs," *IEEE Antennas Wireless Propag. Lett.*, vol. 16, pp. 1985–1989, 2017.

[13] A. Ramachandran, S. Mathew, V. Rajan, and V. Kesavath, "A compact triband quad-element MIMO antenna using SRR ring for high isolation," *IEEE Antennas Wireless Propag. Lett.*, vol. 16, pp. 1409–1412, 2016.

[14] B. L. Dhevi, K. S. Vishvaksenan, and K. Rajakani, "Isolation enhancement in dual-band microstrip antenna array using asymmetric loop resonator," *IEEE Antennas Wireless Propag. Lett.*, vol. 17, pp. 238–241, 2018.

[15] F. Yang and Y. Rahmat-Samii, "Microstrip antennas integrated with electromagnetic band-gap (EBG) structures: A low mutual coupling design for array applications," *IEEE Trans. Antennas Propag.*, vol. 51, no. 10, pp. 2936–2946, Oct. 2003.

[16] H. S. Farahani, M. Veysi, M. Kamyab, and A. Tadjalli, "Mutual coupling reduction in patch antenna arrays using a UC-EBG superstrate," *IEEE Antennas Wireless Propag. Lett.*, vol. 9, pp. 57–59, 2010.

[17] G. Expósito-Domínguez, J.-M. Fernández-Gonzalez, P. Padilla, and M. Sierra-Castañer, "Mutual coupling reduction using EBG in steering antennas," *IEEE Antennas Wireless Propag. Lett.*, vol. 11, pp. 1265–1268, 2012.

[18] M. J. Al-Hasan, T. A. Denidni, and A. R. Sebak, "Millimeter-wave compact EBG structure for mutual coupling reduction applications," *IEEE Trans. Antennas Propag.*, vol. 63, no. 2, pp. 823–828, Feb. 2015.

[19] X. Yang, Y. Liu, Y.-X. Xu, and S.-X. Gong, "Isolation enhancement in patch antenna array with fractal UC-EBG structure and cross slot," *IEEE Antennas Wireless Propag. Lett.*, vol. 16, pp. 2175–2178, 2017.

[20] B. Mohamadzade and M. Afsahi, "Mutual coupling reduction and gain enhancement in patch array antenna using a planar compact electromagnetic bandgap structure," *IET Microw., Antennas Propag.*, vol. 11, no. 12, pp. 1719–1725, Sep. 2016.

[21] H. Wong, K.-L. Lau, and K.-M. Luk, "Design of dual-polarized L-probe patch antenna arrays with high isolation," *IEEE Trans. Antennas Propag.*, vol. 52, no. 1, pp. 45–52, Jan. 2004.

[22] C.-Y. Chiu, C.-H. Cheng, R. D. Murch, and C. R. Rowell, "Reduction of mutual coupling between closely-packed antenna elements," *IEEE Trans. Antennas Propag.*, vol. 55, no. 6, pp. 1732–1738, Jun. 2007.

[23] S. Xiao, M.-C. Tang, Y.-Y. Bai, S. Gao, and B.-Z. Wang, "Mutual coupling suppression in microstrip array using defected ground structure," *IET Microw., Antennas Propag.*, vol. 5, no. 12, pp. 1488–1494, Sep. 2011.

[24] S. Zhang, B. K. Lau, Y. Tan, Z. Ying, and S. He, "Mutual coupling reduction of two PIFAs with a T-shape slot impedance transformer for MIMO mobile terminals," *IEEE Trans. Antennas Propag.*, vol. 60, no. 3, pp. 1521–1531, Mar. 2012.

[25] L. Qu, R. Zhang, and H. Kim, "Decoupling between ground radiation antennas with ground-coupled loop-type isolator for WLAN applications," *IET Microw., Antennas Propag.*, vol. 10, no. 5, pp. 546–552, Apr. 2016.

[26] K. Wei, J.-Y. Li, L. Wang, Z.-J. Xing, and R. Xu, "Mutual coupling reduction by novel fractal defected ground structure bandgap filter," *IEEE Trans. Antennas Propag.*, vol. 64, no. 10, pp. 4328–4335, Oct. 2016.

[27] M.-C. Tang, S. Xiao, B. Wang, J. Guan, and T. Deng, "Improved performance of a microstrip phased array using broadband and ultra-low-loss metamaterial slabs," *IEEE Antennas Propag. Mag.*, vol. 53, no. 6, pp. 31–41, Dec. 2011.

[28] X. M. Yang, X. G. Liu, X. Y. Zhou, and T. J. Cui, "Reduction of mutual coupling between closely packed patch antennas using waveguided metamaterials," *IEEE Antennas Wireless Propag. Lett.*, vol. 11, pp. 389–391, 2012.

[29] Z. Qamar, U. Naeem, S. A. Khan, M. Chongcheawchamnan, and M. F. Shafique, "Mutual coupling reduction for high-performance densely packed patch antenna arrays on finite substrate," *IEEE Trans. Antennas Propag.*, vol. 64, no. 5, pp. 1653–1660, May 2016.

[30] S. Gupta, Z. Briqech, A. R. Sebak, and T. A. Denidni, "Mutual-coupling reduction using metasurface corrugations for 28 GHz MIMO applications," *IEEE Antennas Wireless Propag. Lett.*, vol. 16, pp. 2763–2766, 2017.

[31] S. Zhang and G. F. Pedersen, "Mutual coupling reduction for UWB MIMO antennas with a wideband neutralization line," *IEEE Antennas Wireless Propag. Lett.*, vol. 15, pp. 166–169, 2016.

[32] S. M. Amjadi and K. Sarabandi, "Mutual coupling mitigation in broadband multiple-antenna communication systems using feedforward technique," *IEEE Trans. Antennas Propag.*, vol. 64, no. 5, pp. 1642–1652, May 2016.

[33] M. Farahani, J. Pourahmadazar, M. Akbari, M. Nedil, A. R. Sebak, and T. A. Denidni, "Mutual coupling reduction in millimeter-wave MIMO antenna array using a metamaterial polarization-rotator wall," *IEEE Antennas Wireless Propag. Lett.*, vol. 16, pp. 2324–2327, 2017.

[34] K.-C. Lin, C.-H. Wu, C.-H. Lai, and T.-G. Ma, "Novel dual-band decoupling network for two-element closely spaced array using synthesized microstrip lines," *IEEE Trans. Antennas Propag.*, vol. 60, no. 11, pp. 5118–5128, Nov. 2012.

[35] C.-H. Wu, C.-L. Chiu, and T.-G. Ma, "Very compact fully lumped decoupling network for a coupled two-element array," *IEEE Antennas Wireless Propag. Lett.*, vol. 15, pp. 158–161, 2016.

[36] K. L. Chung and S. Kharkovsky, "Mutual coupling reduction and gain enhancement using angular offset elements in circularly polarized patch array," *IEEE Antennas Wireless Propag. Lett.*, vol. 12, pp. 1122–1124, 2013.

ZHIYUAN CHEN (S'16) received the B.S. degree in electronic science and technology from the Shandong Normal University (SDNU), Jinan, China, in 2015. He is currently pursuing the Ph.D. degree in electronics and communication engineering with Chongqing University, Chongqing, China. His research interests include ultra-wideband antennas, and planar antennas and arrays.

MEI LI (S'15–M'16) received the B.S. degree in electronic information science and technology from the Chengdu University of Information Technology, Chengdu, China, in 2010, and the Ph.D. degree in radio physics from the University of Electronic Science and Technology of China, Chengdu, in 2016. From 2014 to 2016, she was with the Applied Electromagnetics Research Group, University of California at San Diego, San Diego, CA, USA, as a Visiting Graduate. She is currently an Assistant Professor with the School of Microelectronics and Communication Engineering, Chongqing University, China. Her research interests include metasurfaces, antennas, and arrays.

GUO LIU received the Ph.D. degree in radio physics from the Xidian University of China, Xi'an, in 2015. From 2014 to 2015, he was with the EMC laboratory, Research Group, The Pennsylvania State University, USA, as a Visiting Ph.D. Student. He is currently an Engineer with the Science and Technology on Electronic Information Control Laboratory, Chengdu, China. His research interests include antennas and passive detection.

ZHENTIAN WU was born in Anhui, China, in 1994. He received the B.S. degree from the West Anhui University, Luan, China, in 2016. He is currently pursuing the Ph.D. degree in electronics and communication engineering with the School of Microelectronics and Communication Engineering, Chongqing University, China. His current research interests include electrically small antenna and directional antenna and their applications.

MING-CHUN TANG (S'12–M'13–SM'16) received the B.S. degree in physics from the Neijiang Normal University, Neijiang, China, in 2005, and the Ph.D. degree in radio physics from the University of Electronic Science and Technology of China (UESTC), in 2013.

From August 2011 to August 2012, he was with the Department of Electrical and Computer Engineering, The University of Arizona, Tucson, AZ, USA, as a Visiting Scholar. He is currently a Professor with the School of Microelectronics and Communication Engineering, Chongqing University, China. His research interests include electrically small antennas, RF circuits, and metamaterial designs and their applications.

Prof. Tang was a recipient of the Best Student Paper Award in the 2010 International Symposium on Signals, Systems and Electronics (ISSSE2010) held in Nanjing, China. His Ph.D. student received Best Student Paper Award from the IEEE 7th Asia-Pacific Conference on Antennas and Propagation (2018 IEEE APCAP) held in Auckland, New Zealand. He is also the founding Chair of the IEEE AP-S/MTT-S Joint Chongqing Chapter. He serves on the Editorial Boards of several journals, including the IEEE Access, IET Electronics Letters, IET Microwaves, and Antennas and Propagation. He has also served on the review boards of many journals, including the IEEE Transactions on Antennas and Propagation, the IEEE Transactions on Microwave Theory and Techniques, the IEEE Antennas and Wireless Propagation Letters, the IEEE Antennas and Propagation Magazine, the IEEE Microwave and Wireless Components Letters, and many international conferences as a General Chair, a TPC Member, a Session Organizer, and the Session Chair.